Limited bone marrow chimerism impairs thymic cell competition and causes leukemia

Bruna S. P. Oliveira[1]*, Rafael A. Paiva[1]*, Carolina C. Pinto[1], Rita V. Paiva[1], Michelle X. G. Pereira[1], Camila V. Ramos[1], Sara Azenha[1], Tiago Paixão[2], Pedro Faísca[3], Vera C. Martins[1,4,5]§

[1]Lymphocyte Development and Leukemogenesis Laboratory, Gulbenkian Institute for Molecular Medicine, Oeiras, Portugal

[2]Advanced Data Analysis Unit, Gulbenkian Institute for Molecular Institute, Lisbon, Portugal

[3]Histopathology Unit, Gulbenkian Institute for Molecular Institute, Lisbon, Portugal

[4]Faculdade de Medicina da Universidade de Lisboa, Lisbon, Portugal

[5]Institute of Immunology, Ulm University Medical Center, Ulm, Germany

* Equal contribution

§ Corresponding author: Vera C. Martins (email: vera-1.martins@uni-ulm.de)

ORCID: 0000-0001-8717-9709

KEYWORDS

Cell competition, T cell development, Thymus, Thymopoiesis, Thymus autonomy, T cell acute lymphoblastic leukemia, T-ALL, X-linked severe combined immunodeficiency, SCID-X1, Common gamma chain, Hematopoietic stem cell transplantation

ABSTRACT

Cell competition in the thymus is a critical tumor suppressor mechanism that prevents leukemia. Here, we show that suboptimal bone marrow correction of γ_c-deficient mice triggers thymus autonomy and subsequent T cell acute lymphoblastic leukemia (T-ALL). γ_c-deficiency results in severe combined immunodeficiency (SCID) in mice and humans, and correction is achieved by hematopoietic stem and progenitor cell (HSPC) transplantation. Following inefficient bone marrow correction of γ_c-deficient mice, thymus function was intermittent, consistent with sporadic thymic colonization events. Thymocyte composition and phenotype changed, with the appearance of an aberrant TCRβ^-CD4$^+$CD8$^+$ population that preceded leukemia. Leukemia onset and incidence were worsened if HSPCs were pre-cultured to mimic conditions used for gene editing and ameliorated if the hosts could not support thymopoiesis immediately. Lastly, the level of bone marrow reconstitution was crucial to inhibit thymus autonomy. Altogether, our data reveal that inefficient bone marrow correction directly impairs cell competition in the thymus and enables leukemia, underscoring the need to consider and preempt thymus autonomy when treating immunodeficiency.

INTRODUCTION

Cell competition in the thymus is a process that promotes cellular turnover and thereby suppresses leukemia[1]. Cell competition was originally described in *Drosophila*[2], and considers that cell clones of different fitness co-occur in a tissue, meaning that the fittest outcompete less fit cells, thereby contributing to optimal organ function[3]. Cell competition is a fundamental process in embryonic development, hematopoiesis, cardiomyocyte homeostasis in mice, and liver regeneration in rats[4]. It counteracts the pathogenesis of intestinal cancer by promoting the extrusion of transformed epithelial cells into the intestinal lumen[5], and regulates cell growth in human cancer[6] (In the thymus, cell competition favors the turnover and replenishment of a precursor population, thereby providing a constant pool of optimal cells for T lymphocyte differentiation, and this suppresses leukemia[1].

Using an experimental mouse model of thymus transplantation, we showed that young T cell precursors, which recently seeded the thymus, are essential to purge the old, less fit precursors, with longer thymus residency[1]. This occurs at defined stages of T cell differentiation and is not generalized to all thymocytes[7]. If cell competition in the thymus is impaired or abrogated, i.e., if thymus colonization by proficient bone marrow progenitors is blocked, the thymus autonomously sustains T lymphocyte production and export for months – thymus autonomy[8, 9]. But there is a major trade-off: thymus autonomy leads to malignant transformation of T lymphocyte precursors and the onset of T cell acute lymphoblastic leukemia (T-ALL)[1, 10]. The murine disease closely resembles human T-ALL in terms of immunophenotype, pathology, genomic, and genetic alterations[1]. Further similarities between the mouse and human T-ALL were gain-of-function mutations in *Notch1*[11], as well as the expression of *Tal1* and *Lmo2* oncogenes, a molecular hallmark of the largest subgroup of pediatric T-ALL[12, 13]. T-ALL is a particularly aggressive subtype of acute lymphoblastic leukemia that arises from T lymphocyte precursors[14], and accounts for 10-15% of pediatric and 20-25% of adult acute lymphoblastic leukemia (ALL)

cases[15, 16]. In this context, we propose that leukemia emerging from impaired cell competition in the murine thymus follows a conserved process that informs on mechanisms underlying human T-ALL.

Our former results resembled the outcome of gene therapy to correct X-linked SCID-X1 in the early 2000's[17, 18]. SCID-X1 is the most common subtype of severe combined immunodeficiency (SCID), and is caused by loss-of-function mutations in the *common gamma chain* (γ_c) gene[19]. SCID-X1 is lethal if untreated because of the lack of T and NK cells, and non-functional B lymphocytes[20], which render affected baby boys susceptible to recurrent infections and failure to thrive. While bone marrow transplantation is the standard of care[19, 21], this approach is limited by the requirement of compatible donors. Being a monogenetic disease, SCID-X1 is a prime candidate for gene therapy treatment. Indeed, γ_c gene correction by gene therapy delivered the first successful results in the early 2000s, with thymus function effectively established and *de novo* T lymphocyte production[22, 23]. While this achievement speaks in favor of SCID-X1 being a good candidate for gene therapy treatment, there were caveats to this approach. Thymus function was kept active in the treated patients, despite indication that the bone marrow ceased to contribute to thymopoiesis[24], a condition compatible with thymus autonomy. The lack of bone marrow contribution indicates that long-term reconstitution was not reached, or its levels were so low that remained undetected. This was expected because those patients were not myeloablated prior to treatment[22, 23]. After gene therapy, 25% of the treated patients developed T-ALL[18, 25], which was attributed to genotoxicity caused by vector insertion next to oncogenes[26, 27]. We have proposed an alternative explanation: that thymus autonomy triggered leukemia and hypothesize that any condition favoring thymus autonomy is permissive to T-ALL. This notion has received support from two independent studies by others that showed that low level of γ_c-proficient reconstitution in bone marrow chimeras has a high risk of leukemia, independently of gene therapy[28, 29]. SCID-X1 remains an unmet medical need that requires novel therapeutic

approaches. This requires the discovery of the principles underlying bone marrow and thymus communication, and how this controls cell competition and T cell development. Adding to the remarkable efforts taken to develop safe viral vectors for gene therapy, we propose to dissect how the bone marrow correction of γ_c-deficiency determines cell fate decisions in the thymus, i.e., whether normal thymopoiesis or leukemogenesis will be favored. We posit that thymus autonomy and leukemia can result from ineffective thymus colonization by bone marrow progenitors. We show that non-preconditioned γ_c-deficient mice develop T-ALL following transplantation of a limited proportion of wild type hematopoietic stem and progenitor cells (HSPC). Preceding T-ALL, thymopoiesis exhibited several features that were consistent with thymus autonomy: DN3-early were highly proliferative, had increased CD71 expression, and a population of $CD4^+CD8^+$ cells lacking TCRβ expression emerged. The latter population also emerged from *Rag2*$^{-/-}$ donors, that have a developmental block at the DN3-early, prior to giving rise to T-ALL. Finally, we found that the level of bone marrow reconstitution defines its capacity to inhibit thymus autonomy upon hematopoietic stem and progenitor cell (HSPC) transplantation. Collectively, our findings establish thymus autonomy as a thymus-intrinsic property with significant implications for health, underscoring the need to restrain it during manipulation of hematopoiesis and T-lymphocyte development.

RESULTS

Inefficient bone marrow reconstitution causes T cell acute lymphoblastic leukemia (T-ALL)

We have previously shown that thymus autonomy has a high risk of T-ALL[1, 10], and proposed that this conclusion can be extended to every condition triggering thymus autonomy[1, 30]. To test whether T-ALL can emerge from wild type hematopoietic progenitors used to reconstitute the bone marrow of γ_C-deficient mouse hosts in restricted proportions, we injected HSPCs intravenously in a mixture of 10% wild type and 90% $\gamma_C^{-/-}$ into $\gamma_C^{-/-}$ mice[31] without preconditioning (Fig. 1 A). HSPCs were either immediately injected after isolation, or cultured for 16 hours using a cytokine cocktail to mimic the conditions used for gene editing[29] (Fig. 1 A). No genetic manipulation was performed. While T-ALL developed in both conditions, it had a faster onset and higher incidence in the group injected with pre-cultured HSPCs (Fig. 1 B). Specifically, mice injected with pre-cultured HSPCs developed T-ALL with an onset at 20.4 week-post injection and incidence of 75.0%, while mice injected with non-cultured HSPCs had the onset of T-ALL at 36.9 week-post injection and incidence of 46.1% (Fig. 1 B). Although there was some phenotypic variability, leukemias had an immature phenotype and the most common resembled CD8 immature single positive to double positive thymocytes (Fig. 1 C). Consistent with the emergence of T-ALL, the cellularity of thymi and spleens was overly increased as compared to that of healthy wild type controls (Fig. 1 D). Most organs analyzed were infiltrated with T-ALL blasts, with a diffuse neoplastic lymphoid proliferation with multisystemic involvement (Fig. 1 E, F). In the central nervous system, the infiltrates involved the arachnoid and pia mater, extending into the choroid plexus of the fourth ventricle. The bone marrow was completely replaced by a diffuse lymphoid neoplastic population. In the lungs, there was marked perivascular and peribronchiolar infiltration by neoplastic lymphoid cells. The spleen showed extensive lymphoid proliferation with complete obliteration of the normal splenic

architecture. In the liver, lymphoid cells proliferated in a portal distribution, effacing the portal tracts and invading the sinusoidal capillaries. The kidneys exhibited interstitial, capsular, and hilar infiltration by neoplastic lymphoid cells, and similar infiltrates were observed in the subepicardium of the right ventricle and right atrium of the heart. In sum, T-ALL emerged from wild type HSPCs transplanted in restricted proportions into non-irradiated $\gamma_c^{-/-}$ hosts without genetic manipulation. Pre-culturing HSPCs had an impact on disease dynamics by increasing incidence and accelerating the onset of T-ALL.

Inefficient bone marrow reconstitution promotes inter-individual thymic heterogeneity with prevalence of DN3 as the most immature thymocytes

To test whether thymus autonomy preceded T-ALL, we used the same protocol as in Fig. 1A and analyzed the mice at 3-, 9-, and 15-week post-injection. There was considerable heterogeneity in the analyzed thymi among different mice. While thymopoiesis was active in most samples, a minority was composed only of circulating T cells (Fig. 2A, B), consistent with a past wave of thymopoiesis. Total thymus cellularity was highest at 3 weeks and declined thereafter (Fig. 2 C). The most immature CD4/CD8 donor double negative (DN) stages were also phenotypically heterogeneous. The most immature wild type HSPC-derived thymocyte populations, the early T lineage progenitor (ETP) and DN2 were not always detected (Fig. 2 D, E, F). Donor DN3 were detected in most thymi at all time points of analysis (Fig. 2 D, G), and were often the most immature thymocytes present (Fig. 2 D, right plot, and Supplementary Fig.1). This was, in fact, the most common phenotype at all timepoints, corresponding to 73.4%, 52.6%, or 52.6% of the analyzed thymi at 3-, 9- or 15-week post injection, respectively. These data were consistent with a population of DN3 that could self-renew to maintain thymus autonomy[32], but could not be distinguished from a single wave of thymopoiesis. Thymi with CD4+CD8+ thymocytes but without DNs were 13.3%, 15.8 and 42.1% at 3-, 9- or 15-week post injection, respectively. Both

phenotypes are consistent with the occurrence of discrete waves of thymopoiesis at different stages across several thymi, which could be explained by sporadic events of thymus colonization by few hematopoietic progenitors. Thymi where all immature populations were present were 13.3%, 31.6%, 5.3% at 3-, 9- or 15-week post injection, respectively, consistent with recent thymus colonization. Within the DN3-early compartment, the transferrin receptor CD71 is usually expressed by very few cells. Here, there was heterogeneity in CD71 expression. Some samples were identical to controls, but others were similar to the phenotypes described in early stages of thymus autonomy (Fig. 2 H, I, J). Likewise, Ki-67 expression (used as proxy for proliferation) was heterogeneous (Fig. 2 K). This is consistent with sporadic events of colonization, in which different thymi were at different levels of a wave of thymopoiesis, and others retain thymopoiesis autonomously from the DN3-early population. Although cell numbers of DN3-early reduced progressively, the population was detected over time for 15 weeks (Fig. 2 L). Lastly, we searched for an abnormal $CD4^{+}CD8^{+}$ population lacking TCRβ, which precedes leukemia in a thymus transplantation model[32]. Indeed, we found that within the $CD4^{+}CD8^{+}$ cells (Fig. 2 M), TCRβ-negative cells were present at heterogeneous levels, and accumulated in several samples (Fig. 2 N, O). We also analyzed the level of bone marrow engraftment for the presence of donor-derived cells in different hematopoietic progenitor populations (Supplementary Fig. 2A). Although the level of engraftment was very low in the progenitor populations LSK and common lymphoid progenitor (CLP, Supplementary Fig. 2B), we could detect donor-derived cells in these populations for up to 15 weeks post injection. Albeit at extremely low levels, donor-derived cells could be detected within multipotent progenitors 1 (MPP1s) (Supplementary Fig. 2C, D). Surprisingly, myeloid-bias MPP2 and MPP3 also contained donor-derived cells (Supplementary Fig. 2C, D). Altogether, these data confirm that bone marrow reconstitution by few injected HSPCs is extremely inefficient in non-irradiated $\gamma_c^{-/-}$ hosts. Most thymi lacked the

most immature thymocyte populations but DN3 remained, which suggests that thymopoiesis could be kept active as result of persistence of this population, as previously observed[32].

TCRβ$^-$CD4$^+$CD8$^+$ aberrant cells develop from autonomous DN3-early thymocytes

As the former analyses did not permit to accurately distinguish thymus autonomy from discrete waves of thymopoiesis, we sought to minimize cellular complexity in the thymus and test whether DN3-early were sufficient to generate the aberrant TCRβ$^-$CD4$^+$CD8$^+$ cells. We therefore used a mixture of 10% *Rag2*$^{-/-}$ (with or without prior culture) plus 90% $\gamma_c^{-/-}$ HSPCs injected into $\gamma_c^{-/-}$ mice, which were analyzed 9 or 15 weeks later (Fig. 3 A). Thymus cellularity was reduced from the first to the second time point (Fig. 3 B). In line with the previous results, *Rag2*$^{-/-}$ donor DN3 thymocytes were detected at both time points, even in thymi lacking the most immature ETP and DN2 populations (Fig. 3 C, D). TCRβ$^-$CD4$^+$CD8$^+$ cells were detected in all analyzed thymi (Fig. 3 E, F). No differences in relative or absolute cell counts were detected between the thymi from cultured versus non-cultured *Rag2*$^{-/-}$ donors for DN3-early (supplementary Fig. 3 A, B) and TCRβ$^-$CD4$^+$CD8$^+$ cells (supplementary Fig. 3 C, D). Consistent with the results obtained with wild type HSPC donors (Fig. 1), T-ALL also ensued from *Rag2*$^{-/-}$ HSPC, with a total of 9 T-ALLs detected from a total of 27 injected hosts in 4 independent experiments. Many of these mice died from causes unrelated to T-ALL, which precluded construction of a T-ALL-free survival curve. Nevertheless, our results show that *Rag*-deficient thymocytes can bypass the β-selection checkpoint in a scenario of limited HSPC reconstitution of $\gamma_c^{-/-}$ mice, generate TCRβ$^-$CD4$^+$CD8$^+$ cells, and are sufficient to cause T-ALL.

In this context, we propose that the low-level of wild type bone marrow engraftment in the γ_c-deficient bone marrow, together with the low number of thymus seeding progenitors is not sufficient to establish a constant supply of lymphoid progenitors to the thymus, thereby leading

to intermittent events of thymus colonization and T lymphocyte production. To test this hypothesis, we transplanted HSPCs using a mixture of 10% *Tg(Rag2p-GFP)* and 90% $\gamma_c^{-/-}$ into $\gamma_c^{-/-}$ mice which were monitored via blood analyses (Fig. 3 G). *Tg(Rag2p-GFP)* mice[33 27,28] express GFP as a transgene under the *Rag2* promoter, and its expression is maintained for up to 10 days after T cells leave the thymus[34]. In other words, GFP-positive T cells in the blood are recent thymic emigrants and can be taken as a measure of thymus activity. Both B and T GFP-positive cells were detected in the blood at different, non-coincident, time points (Fig. 3 H). Importantly, clear peaks of GFP-positive T lymphocytes in the blood were interspersed with periods where the percentage of GFP-positive T lymphocytes was kept very low to non-detectable (Fig. 3 I). These data demonstrate that T lymphocyte production was not constant overtime and could be jumpstarted even after long periods lacking thymic activity (Fig. 3 H, I, top panels). These refractory periods varied in duration across individual mice, suggesting stochasticity in thymus seeding and subsequent thymopoiesis. In line with the results shown in Fig. 1, these mice developed T-ALL with onset at 29.1 week-post injection and incidence of 66.7% by the end of the observation period (Fig. 3 J). The immunophenotype of these leukemias was heterogeneous, but commonly with an immature CD4+CD8+ profile (Fig. 3 K). Together, these data show that T lymphopoiesis resulting from a low-level chimerism of the bone marrow is intermittent, which can be explained by a stochastic pattern of thymus colonization by rare wild type progenitors, that ultimately culminates in T-ALL.

T-ALL incidence and onset depend on the thymic microenvironment

Former studies using γ_c-deficient[29] or *Rag2*$^{-/-}\gamma_c^{-/-}$ mice[28] reported some differences in T-ALL incidence, and we therefore injected HSPCs in a mixture of pre-cultured 10% wild type plus 90% $\gamma_c^{-/-}$ into *Rag2*$^{-/-}\gamma_c^{-/-}$ recipients (Fig. 4 A). Although T-ALL also emerged in *Rag2*$^{-/-}\gamma_c^{-/-}$ hosts

(Fig. 4 B), it had a later onset (47.9 wk) and lower incidence (22.2%) when compared to the $\gamma_c^{-/-}$ recipients (Fig. 1 B). T-ALL blasts were immature single positive to CD4+CD8+ (Fig. 4 C), and the cellularity of both thymi and spleens was overly enlarged as compared to wild type healthy controls (Fig. 4 D). All analyzed organs were infiltrated with blasts (Fig. 4 E). To test whether $\gamma_c^{-/-}$ and *Rag2*$^{-/-}\gamma_c^{-/-}$ thymi differed in their immediate capacity to support T cell differentiation, we injected 500 000 wild type HSPCs into non-irradiated $\gamma_c^{-/-}$ or *Rag2*$^{-/-}\gamma_c^{-/-}$ mice and analyzed them 3 or 9 weeks later (Fig. 4 F). Differences in total thymus cellularity were notorious between the two groups (Fig. 4 G). While thymopoiesis was evident in $\gamma_c^{-/-}$ thymi 3 weeks after injection, that was not the case in *Rag2*$^{-/-}\gamma_c^{-/-}$ thymi, which could not support thymopoiesis (Fig. 4 G, H). By 9 weeks post injection, both $\gamma_c^{-/-}$ as well as *Rag2*$^{-/-}\gamma_c^{-/-}$ thymi showed CD4+CD8+ thymocytes, although total numbers were significantly lower in *Rag2*$^{-/-}\gamma_c^{-/-}$ hosts (Fig. 4 G). Thymopoiesis was accompanied by structural alterations that could be observed histologically (Fig. 4 I, J, K). While CD4+CD8+ double positive thymocytes occupied cortical areas, CD4+ or CD8+ single positive thymocytes located to the medullas (Fig. 4 I). Structurally, the thymic epithelium plays an important role in supporting thymopoiesis, and we could see obvious differences in epithelial composition and organization between $\gamma_c^{-/-}$ and *Rag2*$^{-/-}\gamma_c^{-/-}$ (Fig. 4 I). While the first had a clear cortex-medulla discrimination, this functional discrimination was absent in *Rag2*$^{-/-}\gamma_c^{-/-}$ mice and only emerged as the experiment progressed in time. No differences were detected in the level of bone marrow engraftment between the two host strains (Supplementary Fig. 4). Altogether, the data support that the initial epithelial structure of the thymus determined the efficiency of thymopoiesis, which ultimately reduced T-ALL incidence.

Next, we used bulk RNAseq to characterize the transcriptome of T-ALL (Supplementary Fig. 5 A). Seven T-ALL samples were compared to control thymocytes and the Principal Component Analysis (PCA) revealed highest separation between control and leukemic cells but could not segregate among the leukemias (Supplementary Fig. 5 B). This suggests that the transcriptome of T-ALL was not influenced by the host, or the culture prior to i.v. injection. Nevertheless, as the number of samples is reduced, our interpretation is also conservative. Differential gene expression (Log2) revealed 3589 genes differentially expressed between T-ALL and controls, with 1150 genes expressed at a lower and 2439 higher levels than the controls (Supplementary Fig. 5 C, D). Among the upregulated genes in T-ALL, we found that *Tal1, Lmo2*, and *Lyl1* were consistently expressed at much higher levels that in control thymocytes (Supplementary Fig. 5 E). While there was also higher expression of *Tlx1, Hhex*, and *Tfrc*, this difference was less pronounced and there was a high degree of interindividual variability (Supplementary Fig. 5 E). At the pathway level, we performed gene set enrichment analysis in the T-ALL samples and found genes for "hallmark Notch signaling" that included *Dll1, Dtx1, Hes1, Fzd1, Fzd5, Fzd7, Heyl, Notch1, Arrb1,* and *Ccnd1*. Genes encoding the "hallmark glycolysis" proteins *Abcb6, Adora2b, Agrn, Artn, B3gnt3, B4galt2, B4galt4, Cacna1h, Chst1, Col5a1, Dsc2, Gpc1, Gpc4, Hs6st2, Ier3, Igfbp3, Isg20, Lhpp, Mertk, Ndst3, Nol3, Pcx, Pkp2, Pygl, Sdc1, Sdc2, Stc1, Tpbg*. "Halmark Heme metabolism" genes were also well represented with 81 genes, and "hallmark p53 pathway" revealed 28 genes. The E2F targets *Cdkn2a* and *Tfrc,* and "hallmark G2M checkpoint" genes *Ccnd1, Meis1, Odc1,* and *Slc7a5* were also enriched in T-ALL. Altogether, our data show that leukemogenesis resulting from limiting bone marrow chimerism depends on a T-cell supportive thymic environment. Once the conditions are met for leukemogenesis, then neither the host, nor pre-culturing cells will dramatically impose on the transcriptional profile or phenotype of T-ALL.

Threshold for thymus autonomy inhibition

Thymus autonomy is a consequence of impairing cell competition in the thymus[1]. Our data supports that limiting the frequency of bone marrow derived progenitors seeding the thymus enables thymus autonomy, which has a high risk of leukemia[10]. Therefore, we sought to determine the threshold of bone marrow engraftment that establishes normal thymopoiesis and prevents thymus autonomy. We generated bone marrow chimeras using lethally irradiated γ_c-deficient mice reconstituted with defined ratios of wild type to $\gamma_c^{-/-}$ HSPCs (Fig. 5 A). In addition, we adoptively transferred 100% or 10% wild type plus 90% $\gamma_c^{-/-}$ HSPCs (either cultured or not cultured) into non-irradiated γ_c-deficient hosts (Fig. 5 A). Three weeks later, all mice were transplanted with wild type thymi and analyzed 5 weeks thereafter (Fig. 5 A). Taking $CD4^+CD8^+$ thymocytes as measurement, we determined their origin and classified thymus grafts into three phenotypes: 1) exhausted, 2) in turnover, or 3) in thymus autonomy (Fig. 5 B). Exhausted thymi were those in which only γ_c-deficient host cells ($CD45.2^+$) were present. Thymus grafts in turnover were composed of wild type HSPC-derived thymocytes ($CD45.1^+$), indicating that wild type bone marrow-derived progenitors replaced the thymus graft thymocytes. Finally, grafts with thymus autonomy were those in which thymocytes of thymus graft origin ($CD45.1^+/CD45.2^+$) persisted. Of note, autonomous thymopoiesis could be dominant in the thymus grafts or co-exist with bone marrow-derived thymopoiesis (Fig. 5 B). The level of bone marrow engraftment was consistent with the proportion of wild type HSPCs injected into lethally irradiated recipients, although some variation was observed (Fig. 5 C). In line with our previous observations, the level of bone marrow engraftment in non-irradiated recipients was extremely low (Fig. 5 C, zoomed in the dashed square). For both irradiated and non-irradiated mice, the frequency of thymus autonomy increased as the percentage of wild type engrafted HSPCs decreased (Fig. 5 D). While thymus autonomy was inhibited in irradiated hosts that received over 50% wild type HSPCs, in non-irradiated hosts thymus autonomy was prevalent even when all transplanted HSPCs were wild type (Fig. 5 D). The analysis of individual mice shows that even

when the relative proportion of injected cells and the experimental conditions are the same, interindividual variability arises, especially when the percentage of wild type engraftment decreases (Supplementary Fig. 6), further supporting that there is stochasticity in thymus seeding. This is most visible among the non-irradiated individuals, where proficient thymus seeding progenitors are extremely reduced, and even γ_C-deficient are capable of thymus seeding (Supplementary Fig. 6). Phenotypically, we define thymus autonomy based on the percentage of CD4+CD8+ cells above 10%[32], meaning that thymus graft derived-thymocytes with ≥10% CD4+CD8+ cells were considered thymus autonomy. We can see that their relative proportion within total CD4+CD8+ thymocytes was mostly represented only in mice with low levels of bone marrow progenitor engraftment (Fig. 5 E), which was also reflected in cellularity (Fig. 5F). Taken together, our data supports that conditioning the hosts optimizes progenitor engraftment, thereby reducing thymus autonomy. A crucial aspect for the capacity of inhibiting autonomy is the relative proportion of wild type HSPCs injected.

DISCUSSION

Here we show that inefficient γ_C-deficiency correction resulting in low level of wild type bone marrow chimerism generates discrete waves of thymopoiesis with intermittent T cell production and export. This was detected in the blood by measuring recent thymic emigrants, which showed that thymus activity occurred in confined time periods that were interspersed by intervals without T cell production. Such observation can only be explained by sporadic events of thymus colonization by wild type hematopoietic progenitors. The estimates for thymus seeding progenitors in wild type mice are in the range of 10 cells per day[35], and each progenitor that reaches the thymus creates one wave of thymopoiesis. The time between two consecutive seeding events is predictably short and ensures constant thymopoiesis. In γ_C-deficient mice with a low-level reconstituted bone marrow, the number of proficient thymus seeding progenitors is expectably lower. Thus, the time between two consecutive waves of wild type thymopoiesis will vary due to stochasticity in thymus seeding, and this impairs thymic cell competition and enables DN3-early self-renewal. Thymus autonomy is thereby triggered, and possibly only suppressed if another wave of thymopoiesis supersedes the thymus before transformation occurs.

In such a scenario, thymus analyses provide snapshots of thymus waves. We consistently detected phenotypic variability documenting waves of thymopoiesis at different stages, as well as thymi only with circulating T cells. Of note, the most frequent phenotype within the CD4-CD8- double negative (DN) stages lacked the most immature ETP to DN2 populations and contained DN3 thymocytes, in line with the capacity of the latter to self-renew[32]. The competition of DN3 thymocytes for thymic niches, and their dependency from interleukin 7 receptor (IL-7r) is well-known in *IL-7rα*$^{-/-}$ mice, which have open niches that can be directly colonized by progenitors injected into the blood stream without the need of irradiation[36]. We previously showed that IL-7r regulates cell competition non-cell autonomously[1, 7]. Further, blocking thymus seeding by thymopoiesis-proficient progenitors hinders thymic cell competition, and triggers

thymus autonomy [8, 9], which later causes T-ALL[1, 10, 30]. This is in line with our current data showing that if thymus seeding is sporadic, the number of thymocytes generated is too low to outcompete DN3 thymocytes with a longer time of thymus residency. In parallel, aberrant CD4+CD8+ thymocytes lacking expression of TCRβ emerge prior to T-ALL onset. Further studies will address how that population expands to generate T-ALL.

Our data is relevant to understand possible consequences of correcting immunodeficiency of SCID-X1 patients[37]. The current standard of care of these patients is a transplant of healthy bone marrow, and no adverse effects have been reported[19, 21, 38]. In the absence of compatible donors, gene therapy might be a solution, as is for another type of SCID, the ADA-SCID[39, 40]. However, the number of gene therapy-corrected cells transplanted might be critical. The efficiency of gene correction of the HSPCs depends on the efficacy of transduction, which means that there is a risk of infusing back a heterogeneous population of progenitors that were not fully corrected. The level of gene correction is not trivial to track in humans, as one cannot use reporter genes. This means that the percentage of cells that were effectively corrected cannot be accurately determined. Importantly, gene therapy requires induction of cell proliferation to transduce HSPCs. Although the goal is to expand cell number without losing multipotency, it is likely that cell culture interferes with HSPC function. In line with this possibility, T cells were faster at being produced in a SCID-X1 patient cohort treated by gene therapy as compared with a cohort receiving haploidentical hematopoietic stem cell transplantation[41]. Our data show that mouse HSPCs cultured overnight change, and the time to T-ALL onset is reduced and incidence increased. This suggests that cultured HSPCs are less effective to home to the bone marrow, that they lose some multipotency and/or generate more differentiated progeny. In either case, if such changes occur in a gene therapy setting, then the effective number of HSPC with capacity for long term engraftment is probably reduced. Finally, although opening the bone marrow niches

bear significant risks for the patient, it also ensures more efficient engraftment, and therefore lower risk of thymus autonomy and leukemia.

It is noteworthy that the thymocyte population involved in cell competition is the same that has self-renewal potential. Such property is likely to have a physiological function that we have not yet found. One possibility could be that DN3-early self-renewal potential is associated to β-selection, optimizing the probability to generate a productive TCRβ rearrangement. In any case, DN3-early cells have been reported to self-renew prior to full T-ALL onset in transgenic mouse models induced by either *Lmo2*[42], or *Lmo1* plus *Tal1*[43] overexpression. This property seems to confer the DN3-early population with characteristics of a super-competitor[44], suggestive that thymocyte self-renewal could be a common mechanism underlying T-ALL initiation[45]. In fact, *LMO2* activation is considered an initiating event in human T-ALL[46]. These examples point at the DN3-early as a population that must be kept in check, and we consider that cell competition is crucial in that respect. At steady state, young DN3-early are constantly outcompeted by young cells with less time of thymus residency. Those with shorter time of thymus residency are more fit than the ones dwelling in the thymus for longer time. If, however, these young precursors do not reach the thymus in sufficient numbers to outcompete the older DN3-early, the latter persist, self-renew, and cause leukemia. Further work will require uncovering the molecular regulation of cell competition in the thymus.

Collectively, our data reveal that DN3-early thymocytes possess an intrinsic capacity for self-renewal, and highlight the physiological cost of this property when bone marrow correction of γ_C-deficiency falls below the threshold required to restore effective thymopoiesis. It is noteworthy that adult hematopoietic progenitors are capable to generate thymocytes with self-renewal potential, as our former work had only demonstrated this property in newborn thymocytes. Using a mouse model of limited bone marrow reconstitution, we show that cell competition in the thymus is a fundamental quality control mechanism that suppresses malignant

transformation. Ultimately, our findings indicate that any condition impairing thymic cell competition and triggering thymus autonomy has a high risk of malignant transformation and leukemia.

ONLINE METHODS

Mice

All mice were maintained and bred at Gulbenkian Institute of Molecular Medicine (Oeiras), former Instituto Gulbenkian de Ciência. C57BL/6J (CD45.2^{+}) were in a colony frequently refreshed by mice imported from Charles River. B6.SJL-Ptprc3^{a} (CD45.1^{+}, here termed B6.SJL), stock #002014, were purchased from The Jackson Laboratory and kept in a colony at IGC. $\gamma_c^{-/-}$ [31], JAX stock #003174 were purchased from The Jackson Laboratory. *Rag2*$^{-/-}\gamma_c^{-/-}$ mice were obtained by crossing *Rag2*$^{-/-}$[47] and $\gamma_c^{-/-}$ mice, both in B6 background, as previously described[10]. Mice of both genders were used at an age of 4 to 8 weeks as recipients and kept in individually ventilated cages in specific pathogen-free (SPF) conditions. All experiments were conducted in compliance with Portuguese and European laws and approved by the internal Animal Welfare Office (ORBEA-GIMM) and *Direção Geral de Alimentação e Veterinária (DGAV)*.

Hematopoietic stem and progenitor cell transplantation

Bone marrow cells from 6- to 8-week-old B6.SJL or B6 (CD45.1^{+} or CD45.2^{+}, wild type) or *Rag2*$^{-/-}$and $\gamma_c^{-/-}$ (CD45.2^{+} or CD45.1^{+}) were incubated with biotinylated antibodies against CD3, CD4, CD8, CD11b, CD11c, CD19, Gr-1, NK1.1 and Terr119 and depleted of lineage^{+} cells by magnetic separation using Biotin Binder Dynabeads (Thermo Fisher Scientific). Depending on the experiment, cells were either directly injected intravenously, or pre-cultured and then injected into the tail vein. Where indicated, cells were cultured for 16 hours at one million lineage-depleted cells per well in 24-well plates in StemPan Serum-Free Expansion Medium (Stem cell technologies, 096000) containing 200 ng/mL vaccinia virus B18R protein (Biovision, 8016-10 for the first set of experiments, AcroBiosystems, B1R-H52H6 for the latest, without noted differences) and the following cytokines from PeproTech: Flt3L (100 ng/mL), SCF

(100 ng/mL), TPO (50 ng/mL) and IL-3 (20 ng/mL). Injected cells consisted of a mixture of a total of $1x10^6$ cells composed of 10% wild type ($CD45.1^+$ or $CD45.2^+$) and 90% $\gamma_c^{-/-}$ ($CD45.1^+$ or $CD45.2^+$) cells. Recipient mice were $\gamma_c^{-/-}$ ($CD45.1^+$ or $CD45.2^+$) or *Rag2*$^{-/-}\gamma_c^{-/-}$ ($CD45.1^+$ or $CD45.2^+$). Mice were used as $CD45.1^+$ or $CD45.2^+$ for donor/host discrimination, without noted functional differences for whether donors were $CD45.1^+$ or $CD45.2^+$. For Fig. 3, Femurs and tibias from Tg(*Rag-GFP)* mice[33] were shipped from ICVS, Braga, to IGC at 4ºC overnight and bone marrow single cell suspension were prepared and transplanted in the morning for the 1st experiment. For experiments depicted in Fig. 5, mice were preconditioned by irradiation (600 rad), as indicated, prior to injection.

Blood analyses

Mice were periodically bled from the submandibular vein to assess peripheral reconstitution and/or to screen for leukemia. Blood was collected into PBS with 1.6 mg/ml EDTA and erythrocytes were lysed using Gey's solution before staining with appropriate antibodies.

Thymus transplants

Thymi from newborn mice were collected and thymic lobes were split. Recipient mice were grafted under the kidney capsule with two lobes, placed into opposing extremities of the kidney. Mice were kept anesthetized with Xylazine (16 mg/kg) and Ketamine (100 mg/kg). *Rag2*$^{-/-}\gamma_c^{-/-}$ or $\gamma_c^{-/-}$ ($CD45.2^+$) recipients of both genders with 5 to 7 weeks were used and thymus donors were wild type ($CD45.1^+CD45.2^+$).

Flow cytometry

Organs were collected and cell suspensions were prepared in PBS with 2% FBS. Cells were blocked with mouse IgG (Jackson laboratories) and then stained with the antibodies against the

following: CD3 (clone 145-2C11; conjugated to APC-Cy7), CD4 (GK1.1; PE, PE-Cy7, BV421, BV605 or BV650), CD8 (53-6.7; FITC, PerCP-Cy5.5, APC Fire 750 or BV711,), CD11b (M1/70; APC), CD19 (6D5; FITC or PE-Cy7), CD25 (PC61; BV605 or FITC), CD44 (IM7; BV711, eFluor450, FITC or PerCP-Cy5.5), CD48 (HM48-1; APC). CD71 (RI7217; FITC), CD150 (TC15-12F12.2; BV605), Gr-1 (RB6-8C5; PE or APC), Kit (2B8; APC or APC-Cy7), Ly6D (49-H4; FITC), Flt3 (A2F10; PE), IL-7r (A7R34; PE-Cy7), Sca-1 (D7; PercP-Cy5.5), CD45.1 (A20; FITC, PE, PE-Cy7, APC, BV421 or BV650) and CD45.2 (104; FITC, PE, APC, APC-Cy7, Pacific Blue or BV711), all from BioLegend. The lineage mix consisted of CD3 (145-2C11), CD4 (GK1.1), CD8 (53-6.7), CD11b (M1/70), CD11c (N418), CD19 (6D5), Gr-1 (RB6-8C5), NK1.1 (PK136) and Ter119 (TER-119), all conjugated to biotin and from BioLegend. Biotinylated antibodies were recognized by streptavidin conjugated to BV785 (BioLegend). Dead cell exclusion was performed using Zombie Pacific Orange (BioLegend). Intracellular staining against Ki-67 (16A8; AF700) and TCRβ (H57-597; AF647 or BV711), from BioLegend was performed with True-Nuclear Transcription Factor Buffer Set (BioLegend). Samples were acquired in a BD LSRFortessa X-20 analyzer and analyzed on FlowJo 10.10.0.

Histopathology

Histological analysis was performed at the Histopathology Facility of the GIMM Institute. Briefly, samples were fixed in 10% neutral-buffered formalin for a minimum of 48 hours at room temperature, except the brain that was fixed for 1 week. Samples were processed automatically (Leica HistoCore Pearl), embedded in paraffin, and sectioned at 3 µm. Sections were mounted on glass slides and stained with hematoxylin and eosin (H&E) following standard protocols. Slides were analyzed with a DMLB2 microscope (Leica), and images were acquired with a DFC320 camera (Leica) and NanoZoomer-SQ Digital slide scanner (Hamamatsu Photonics).

Immunohistology

Thymi were collected and cryopreserved in OCT. Sections (8 µm thick) were obtained using a Leica Cryostat CM 3050 S, dehydrated with acetone and stored at -80 ºC until use. Sections were incubated with DAPI and mouse IgG, stained overnight with rabbit Keratin 5 (Poly19055), Keratin 8-Alexa647 (1E8), CD11c-Bio (N418), CD4-Alexa647 (GK1.5) and CD8-Alexa488 (53-6.7), followed by Streptavidin-Cy3 and anti-rabbit Alexa488, as appropriate. Slides were mounted with Fluoromount G medium (Invitrogen) and images were acquired on a Zeiss Axio Imager with Apotome 2 microscope. Fiji was used for image treatment and QuPath for analysis and quantification.

RNA isolation and sequencing

Cell pellets containing 5 million or 20 million cells were prepared from leukemia samples and stored as dry pellets at −80°C until use. Total RNA was then isolated by lysing the cells with Trizol (Invitrogen), followed by RNA phase separation with trichloromethane/chloroform (Carl Roth), precipitation with 2-propanol (VWR BDH Chemicals), and dilution in RNAse-free water. Quality control and RNA concentration was determined in a Fragment analyzer. The isolated RNA were stored at −80°C until sequencing. Sequencing was performed by Novogene Co., Ltd.. For sequencing, first messenger RNA was purified from total RNA using poly-T oligo-attached magnetic beads. After fragmentation, the first strand cDNA was synthesized using random hexamer primers followed by the second strand cDNA synthesis. The library was ready after end repair, A-tailing, adapter ligation, size selection, amplification, and purification. The library constructed was checked with Qubit and real-time PCR for quantification and bioanalyzer for size distribution detection. Quantified libraries were pooled, based on the effective concentration and targeted data amount, and sequenced on Illumina platforms.

Bioinformatics Analyses

Quality control (QC) and filtering of raw sequencing reads were performed using fastp with default parameters. The processed reads were then aligned to the genome (version 111) using STAR with default settings. Gene-level counts were subsequently obtained with FeatureCounts, applying default parameters optimized for paired-end data. The resulting read counts were analyzed in R using DESeq2[48]. Genes with average read counts less than 5 were filtered out. For PCA analysis, the data were transformed using DESeq2's variance stabilizing transformation and used the top 500 more variable genes. Differential gene expression analysis was conducted using the DESeq2 package in R. Pathway analysis was performed with a gene set enrichment analysis (GSEA) using the Hallmarks Gene Set collection.

ACKNOWLEDGEMENTS

This work was supported by the "La Caixa" Foundation grant LCF/PR/HR22/52420023 to VCM, the Portuguese National Research Council (Fundação para a Ciência e Tecnologia [FCT] Grant PTDC/MED-IMU/3649/2021 to VCM and Instituto Gulbenkian de Ciência (IGC) of the Calouste Gulbenkian Foundation. VCM was supported by an individual contract awarded by FCT (CEECIND/03106/2018). CP is a PhD student of the IGC Integrative Biology and Biomedicine (IBB) PhD Program and is supported by an individual FCT PhD Fellowship ref. UI/BD/154901/2023. RAP and CVR were PhD students of the IBB PhD Program and were supported by individual FCT PhD Fellowships refs. PD/BD/114341/2016 and PD/BD/139190/2018, respectively. We thank Margarida Correia-Neves for the *Tg(Rag2p-GFP)* bone marrow cells. We thank Olivier Joffre and Pamela Fink for the *Tg(Rag2p-GFP)* mice. We thank the team of Animal House Facility, and the Flow Cytometry Facility for their outstanding support, and acknowledge the Microscopy, Histopathology, Genomics and Bioinformatics Units of GIMM in supporting this work.

AUTHOR CONTRIBUTIONS

BSPO e RAP designed and performed experiments, analyzed data and wrote the manuscript. CCP performed experiments and analyzed RNA seq data; RVP, CVR, SA performed and analyzed experiments; MXGP, performed RNA experiments. P.F. did the histopathological assessment of the leukemic samples, T.P. did the preliminary bioinformatics analysis of the RNAseq data. VCM conceived the study, designed research and experiments, analyzed data and wrote the manuscript. All authors edited and contributed to the final version of the manuscript.

COMPETING INTERESTS STATEMENT

The authors have no conflicts of interests.

FIGURE LEGENDS

Figure 1. Limiting bone marrow chimerism causes T-ALL. A) 10^6 HSPCs in a mixture of 10% wild type plus 90% $\gamma c^{-/-}$, were i.v. injected into non-preconditioned $\gamma c^{-/-}$ mice. One group of mice received HSPCs that were previously cultured for 16 hours as indicated. CD45.1 and CD45.2 were used to distinguish donor/host-derived cells. B) Percentage of T-ALL free mice over time. C) Representative CD4CD8 profiles of wild type control thymocytes and T-ALL samples. Numbers show percentage of cells in each quadrant, gated on donor cells for T-ALL. D) Cellularity of thymi and spleens in controls and mice with T-ALL. Each dot represents one mouse, and the lines represent the medians. E) Representative sections of the indicated organs stained with hematoxylin and eosin. Scale bars: 1 mm. F) Overview of the leukemic infiltration in T-ALL-bearing mice.

Figure 2. Limiting bone marrow chimerism associates with phenotypic heterogeneity and hallmarks of thymus autonomy. A) Representative examples of the most extreme phenotypes obtained for the donor CD4/CD8 profile, following bone marrow transplantation. Examples are from 9-week post-transplantation. Numbers show percentage of cells in each quadrant. B) Quantification of thymi with or without donor-derived thymopoiesis 3-, 9- and 15-week post-transplantation. Numbers on top of the columns indicate the number of mice analyzed. C) Thymus cellularity at the indicated time points. D) Representative examples of the phenotypes observed among the most immature donor DN thymocyte populations. Examples are from 9 weeks after HSPC transplantation, and cells were pre-gated as negative for CD4, CD8, Lin-markers. E-G) Absolute cell counts of the indicated populations 3-, 9- and 15-week post-injection. H) Donor DN3 thymocytes are shown for the intracellular expression of TCRβ and CD71. I) Example of donor DN3-early samples 9-wk after injection (red) or a control (grey). J) Quantification of CD71+ cells in DN3-early (DN3e) cells. K) Quantification of Ki67 high-expressing donor DN3-early. L) Cellularity of donor DN3-early. M) Quantification of donor derived $CD4^+CD8^+$ double positive (DP) cells. N) Representative example of one thymus depicting $TCR\beta^-CD4^+CD8^+$. O) Quantification of TCRβ-negative cells in $CD4^+CD8^+$ donor thymocytes. In C), E), F), G), L) and M) lines represent the medians, and in J), K) and O) lines represent means. In all, each circle represents one mouse. Control samples refer to wild type, non-manipulated mice. Data are from 10 independent experiments containing a total n =62.

Figure 3. TCRβ$^-$CD4$^+$CD8$^+$ cells and intermittent thymopoiesis precede T-ALL. A) 10^6 HSPCs in a mixture of 10% *Rag2*$^{-/-}$ plus 90% $\gamma c^{-/-}$, were i.v. injected into non-preconditioned $\gamma c^{-/-}$ mice, which were analyzed 9- and 15-week later. CD45.1 and CD45.2 were used to distinguish donor/host-derived cells. B) Thymus cellularity after HSPC transplantation. Each dot represents one mouse, and the lines represent the medians. C) Representative examples of samples donor DN populations. Cells were pre-gated as negative for CD4, CD8, Lin-markers. D) Quantification of the thymi with DN3 thymocytes. E) Representative examples of thymi with a population of donor CD4+CD8+. F) Quantification of samples with CD4+CD8+ double positive (DP-like) population. Data in E-F is cumulative from 8 independent experiments with n=4-8 mice/experiment and a total of n=20 without culture, and n=24 with culture. G) 10^6 HSPCs in a mixture of 10% *Tg(Rag2-GFP)* plus 90% $\gamma c^{-/-}$, were i.v. injected into non-preconditioned $\gamma c^{-/-}$ mice, which were periodically bled thereafter. H) Quantification of GFP-positive cells in the blood, depicting the correspondent proportion of T and B cells, over time. Each graph represents one mouse. I) Quantification of GFP-positive cells in the blood, as percentage of total T cells, and the correspondent proportion of CD4+ and CD8+ T cells, over time. Each graph represents the same mice in H. J) Percentage of T-ALL-free over time. K) Representative CD4/CD8 FACS profile of a T-ALL. Numbers show percentage of cells in each quadrant. Data in A-F are from 8 independent experiments containing n =4-8/experiment. Data in H-K are from one individual experiment, n=10.

Figure 4. The thymic microenvironment determines T-ALL incidence and onset. A) 10^6 HSPCs in a mixture of 10% wild type plus 90% $\gamma c^{-/-}$, were cultured for 16 hours and i.v. injected into non-preconditioned *Rag2*$^{-/-}\gamma c^{-/-}$ mice. CD45.1 and CD45.2 were used to distinguish donor/host-derived cells. B) Percentage of T-ALL free over time. C) CD4CD8 profile for one T-ALL sample. Numbers show percentage of cells in each quadrant, gated on donor cells for T-ALL. D) Cellularity of thymi and spleens in control and mice with T-ALL. Each dot represents

one mouse. E) Representative sections of the indicated organs stained with hematoxylin and eosin. Scale bars: 1mm. F) 500 000 wild type HSPCs were transplanted into non-preconditioned $\gamma c^{-/-}$ (n=10) or *Rag2*$^{-/-}\gamma c^{-/-}$ (n=10) recipients and the thymi of the mice were analyzed 3 or 9 weeks after injection. One lobe was used for flow cytometry (H) and the other for histology (I). G) Thymus cellularity, where each dot represents one mouse, and the lines represent the medians. H) Representative examples of CD4CD8 profiles, pre-gated on donor cells. I) Immunohistology analysis of the indicated mice and timepoints. Pseudocolors are: CD4 (blue), CD8 (green), CD11c (magenta), keratin 5 (green), keratin 8 (red). Scale bar = 250 µm. J) Quantification of the thymus area (µm^2) of the analyzed immunohistology sections. Each dot represents one thymus section, each bar shows the mean. K) Percentage of cortex and medullary areas within each thymic section. Data in G-K are from 2 independent experiments containing n =4-6/experiment.

Figure 5. Threshold for inhibition of thymus autonomy. A) 10^6 HSPCs in the indicated percentages of wild type (CD45.1$^+$) to $\gamma c^{-/-}$ (CD45.2$^+$) cells were i.v. injected into hosts (CD45.2$^+$) that were either lethally irradiated (total body irradiation, TBI) or untreated. For the non-irradiated hosts, one group received pre-cultured cells, and the other non-cultured cells. Three weeks later, mice were transplanted with newborn wild type thymi (CD45.1$^+$/CD45.2$^+$) and analyzed 5 weeks thereafter. B) Representative examples of phenotypic outcomes depicting the origin of the cells. C) Effective level of engraftment in bone marrow progenitors measured in LSK. Blue highlighted region in the main graph is zoomed in above. D) Percentage of thymi exhausted, autonomous or in turnover in the indicated groups. Numbers on the bars correspond to the thymus grafts analyzed with the corresponding phenotype. E) Relation between effective engraftment in bone marrow LSK (x-axis) and the percentage of thymus graft-derived CD4CD8 double positive thymocytes. F) Relation between absolute cell counts of thymus graft-derived CD4CD8 double positive thymocytes and engraftment in bone marrow LSK. Shown is cumulative data from 5 independent experiments where hosts were $\gamma c^{-/-}$ (n=44) or *Rag2*$^{-/-}\gamma c^{-/-}$ (n=71) in total. No differences were observed among the groups of irradiated mice.

SUPPLEMENTARY FIGURE LEGENDS

Supplementary Figure 1. Quantification of donor-derived cells in bone marrow progenitors. Mice in Fig. 2 were analyzed for the origin of cells of their bone marrow progenitors. A) Gating strategy. B, C) Quantification of donor-derived cells in the indicated populations. Each dot represents a mouse and the line is the mean. D) Average ± Standard Deviation of the data shown in B, D.

Supplementary Figure 2. Quantification of thymus and bone marrow cells. Mice in Fig. 3 A were analyzed for the A) percentage and B) cell counts of DN3, and C) percentage and D) cell counts of CD4+CD8+ double positive-like (DP-like) cells. (E to J) The percentage of the indicated donor populations in live bone marrow cells was determined for the mice that received 10^6 cultured HSPCs (E-G, plots with red datapoints) and for the mice that received 10^6 non-cultured HSPCs (H-J, plots with red datapoints). Each square represents a mouse.

Supplementary Figure 3. Quantification of bone marrow engraftment. Mice in Fig. 4 F were analyzed for the percentage of donor cells in A) LSK, B) CLP, C) LMPP, and D LSK Flt3-negative. Red dots represent data from $\gamma c^{-/-}$ hosts, and blue dots from *Rag2*$^{-/-}$ $\gamma c^{-/-}$ hosts.

Supplementary Figure 4. Characterisation of T-ALL transcriptomics. A) T-ALL arising after injection of 10^6 HSPCs in a mixture of 10% wild type plus 90% as described in Fig. 1A and 4 A were analyzed by RNAseq. B) PCA for global gene expression of T-ALL samples in red (n = 7), and wild-type thymocytes in black (n=3). Symbols reflect the origin of the samples as indicated. C) Volcano plot depicting differentially expressed genes between T-ALL and wild-type thymocytes. Red represents genes expressed at higher level in T-ALL, and blue represents genes with lower expression level in T-ALL as compared to wild type thymocytes. D) Heatmap

depicts differentially expressed genes between T-ALL and wild-type thymocytes with corrected $p < 0.01$ and a $\log_2$ fold change ≥ 2. E) Transcript abundance (counts pre million) for the indicated genes obtained from normalized transcriptome data. Each dot represents one mouse, and the lines represent the means. F-H) T-ALL samples described in (A, red dots) were compared to T-ALL samples obtained by transplantation of a wild thymus into a *Rag2*$^{-/-}$$\gamma_c^{-/-}$ host (green dots), as described previously[1, 10] F) PCA of all T-ALL samples and wild type thymocytes. G) PCA of all T-ALL samples. H) Vulcano plot depicting differential gene expression between the two types of T-ALL, highlighting B cell-related genes.

Supplementary Figure 5. Thymus composition of individual mice. Thymus grafts of the mice depicted in Fig. 5 A were analyzed for the origin of the thymocytes within the CD4CD8 double positive population. Each bar represents one mouse, and the thymocyte origin is depicted by different colors, as shown, corresponding to the indicated percentages. Data shown is from one experiment, out of five independent experiments.

REFERENCES

1. Martins, V.C. *et al.* Cell competition is a tumour suppressor mechanism in the thymus. *Nature* **509**, 465–470 (2014).

2. Moreno, E. Is cell competition relevant to cancer? *Nature reviews. Cancer* **8**, 141–147 (2008).

3. Merino, M.M., Levayer, R. & Moreno, E. Survival of the Fittest: Essential Roles of Cell Competition in Development, Aging, and Cancer. *Trends Cell Biol* **26**, 776–788 (2016).

4. Claveria, C. & Torres, M. Cell Competition: Mechanisms and Physiological Roles. *Annu Rev Cell Dev Biol* **32**, 411–439 (2016).

5. Kon, S. *et al.* Cell competition with normal epithelial cells promotes apical extrusion of transformed cells through metabolic changes. *Nature cell biology* **19**, 530–541 (2017).

6. Madan, E. *et al.* Flower isoforms promote competitive growth in cancer. *Nature* **572**, 260–264 (2019).

7. Ramos, C.V. *et al.* Cell Competition, the Kinetics of Thymopoiesis, and Thymus Cellularity Are Regulated by Double-Negative 2 to 3 Early Thymocytes. *Cell reports* **32**, 107910 (2020).

8. Martins, V.C. *et al.* Thymus-autonomous T cell development in the absence of progenitor import. *J Exp Med* **209**, 1409–1417 (2012).

9. Peaudecerf, L. *et al.* Thymocytes may persist and differentiate without any input from bone marrow progenitors. *J Exp Med* **209**, 1401–1408 (2012).

10. Ballesteros-Arias, L. *et al.* T Cell Acute Lymphoblastic Leukemia as a Consequence of Thymus Autonomy. *J Immunol* **202**, 1137–1144 (2019).

11. Weng, A.P. *et al.* Activating mutations of NOTCH1 in human T cell acute lymphoblastic leukemia. *Science* **306**, 269–271 (2004).

12. Ferrando, A.A. *et al.* Gene expression signatures define novel oncogenic pathways in T cell acute lymphoblastic leukemia. *Cancer cell* **1**, 75–87 (2002).

13. Homminga, I. *et al.* Integrated transcript and genome analyses reveal NKX2-1 and MEF2C as potential oncogenes in T cell acute lymphoblastic leukemia. *Cancer cell* **19**, 484–497 (2011).

14. Van Vlierberghe, P. & Ferrando, A. The molecular basis of T cell acute lymphoblastic leukemia. *J Clin Invest* **122**, 3398–3406 (2012).

15. Pui, C.H., Relling, M.V. & Downing, J.R. Acute lymphoblastic leukemia. *N Engl J Med* **350**, 1535–1548 (2004).

16. Pagliaro, L. *et al.* Acute lymphoblastic leukaemia. *Nat Rev Dis Primers* **10**, 41 (2024).

17. Hacein-Bey-Abina, S. *et al.* A serious adverse event after successful gene therapy for X-linked severe combined immunodeficiency. *N Engl J Med* **348**, 255–256 (2003).

18. Hacein-Bey-Abina, S. *et al.* LMO2-associated clonal T cell proliferation in two patients after gene therapy for SCID-X1. *Science* **302**, 415–419 (2003).

19. Antoine, C. *et al.* Long-term survival and transplantation of haemopoietic stem cells for immunodeficiencies: report of the European experience 1968-99. *Lancet* **361**, 553–560 (2003).

20. Noguchi, M. *et al.* Interleukin-2 receptor gamma chain mutation results in X-linked severe combined immunodeficiency in humans. *Cell* **73**, 147–157 (1993).

21. Gennery, A.R. *et al.* Transplantation of hematopoietic stem cells and long-term survival for primary immunodeficiencies in Europe: entering a new century, do we do better? *The Journal of allergy and clinical immunology* **126**, 602–610 e601–611 (2010).

22. Cavazzana-Calvo, M. *et al.* Gene therapy of human severe combined immunodeficiency (SCID)-X1 disease. *Science* **288**, 669–672 (2000).

23. Hacein-Bey-Abina, S. *et al.* Sustained correction of X-linked severe combined immunodeficiency by ex vivo gene therapy. *N Engl J Med* **346**, 1185–1193 (2002).

24. Hacein-Bey-Abina, S. *et al.* Efficacy of gene therapy for X-linked severe combined immunodeficiency. *N Engl J Med* **363**, 355–364 (2010).

25. McCormack, M.P., Forster, A., Drynan, L., Pannell, R. & Rabbitts, T.H. The LMO2 T-cell oncogene is activated via chromosomal translocations or retroviral insertion during gene therapy but has no mandatory role in normal T-cell development. *Mol Cell Biol* **23**, 9003–9013 (2003).

26. Hacein-Bey-Abina, S. *et al.* Insertional oncogenesis in 4 patients after retrovirus-mediated gene therapy of SCID-X1. *J Clin Invest* **118**, 3132–3142 (2008).

27. Howe, S.J. *et al.* Insertional mutagenesis combined with acquired somatic mutations causes leukemogenesis following gene therapy of SCID-X1 patients. *J Clin Invest* **118**, 3143–3150 (2008).

28. Ginn, S.L. *et al.* Limiting Thymic Precursor Supply Increases the Risk of Lymphoid Malignancy in Murine X-Linked Severe Combined Immunodeficiency. *Mol Ther Nucleic Acids* **6**, 1–14 (2017).

29. Schiroli, G. *et al.* Preclinical modeling highlights the therapeutic potential of hematopoietic stem cell gene editing for correction of SCID-X1. *Sci Transl Med* **9**, eaan0820 (2017).

30. Paiva, R.A., Ramos, C.V. & Martins, V.C. Thymus autonomy as a prelude to leukemia. *FEBS J* **285**, 4565–4574 (2018).

31. Cao, X. *et al.* Defective lymphoid development in mice lacking expression of the common cytokine receptor gamma chain. *Immunity* **2**, 223–238 (1995).

32. Paiva, R.A. *et al.* Self-renewal of double-negative 3 early thymocytes enables thymus autonomy but compromises the beta-selection checkpoint. *Cell reports* **35**, 108967 (2021).

33. Yu, W. *et al.* Continued RAG expression in late stages of B cell development and no apparent re-induction after immunization. *Nature* **400**, 682–687 (1999).

34. Boursalian, T.E., Golob, J., Soper, D.M., Cooper, C.J. & Fink, P.J. Continued maturation of thymic emigrants in the periphery. *Nat Immunol* **5**, 418–425 (2004).

35. Zietara, N. *et al.* Multicongenic fate mapping quantification of dynamics of thymus colonization. *J Exp Med* **212**, 1589–1601 (2015).

36. Prockop, S.E. & Petrie, H.T. Regulation of thymus size by competition for stromal niches among early T cell progenitors. *J Immunol* **173**, 1604–1611. (2004).

37. Ginn, S.L., McCormack, M.P. & Alexander, I.E. Thymocyte self-renewal and oncogenic risk in immunodeficient mouse models: relevance for human gene therapy clinical trials targeting haematopoietic stem cell populations? *Mamm Genome* **29**, 771–776 (2018).

38. Castagnoli, R., Delmonte, O.M., Calzoni, E. & Notarangelo, L.D. Hematopoietic Stem Cell Transplantation in Primary Immunodeficiency Diseases: Current Status and Future Perspectives. *Front Pediatr* **7**, 295 (2019).

39. Aiuti, A., Roncarolo, M.G. & Naldini, L. Gene therapy for ADA-SCID, the first marketing approval of an ex vivo gene therapy in Europe: paving the road for the next generation of advanced therapy medicinal products. *EMBO Mol Med* **9**, 737–740 (2017).

40. Ferrua, F. & Aiuti, A. Twenty-Five Years of Gene Therapy for ADA-SCID: From Bubble Babies to an Approved Drug. *Hum Gene Ther* **28**, 972–981 (2017).

41. Touzot, F. *et al.* Faster T-cell development following gene therapy compared with haploidentical HSCT in the treatment of SCID-X1. *Blood* **125**, 3563–3569 (2015).

42. McCormack, M.P. *et al.* The Lmo2 oncogene initiates leukemia in mice by inducing thymocyte self-renewal. *Science* **327**, 879–883 (2010).

43. Gerby, B. *et al.* SCL, LMO1 and Notch1 reprogram thymocytes into self-renewing cells. *PLoS Genet* **10**, e1004768 (2014).

44. Abdulla, H.D. *et al.* Overexpression of Lmo2 initiates T-lymphoblastic leukemia via impaired thymocyte competition. *J Exp Med* **220** (2023).

45. Boehm, T. Self-renewal of thymocytes in the absence of competitive precursor replenishment. *J Exp Med* **209**, 1397–1400 (2012).

46. Boehm, T., Foroni, L., Kaneko, Y., Perutz, M.F. & Rabbitts, T.H. The rhombotin family of cysteine-rich LIM-domain oncogenes: distinct members are involved in T-cell translocations to human chromosomes 11p15 and 11p13. *Proc Natl Acad Sci U S A* **88**, 4367–4371 (1991).

47. Shinkai, Y. *et al.* RAG-2-deficient mice lack mature lymphocytes owing to inability to initiate V(D)J rearrangement. *Cell* **68**, 855–867 (1992).

48. Love, M.I., Huber, W. & Anders, S. Moderated estimation of fold change and dispersion for RNA-seq data with DESeq2. *Genome Biol* **15**, 550 (2014).

Figure 1

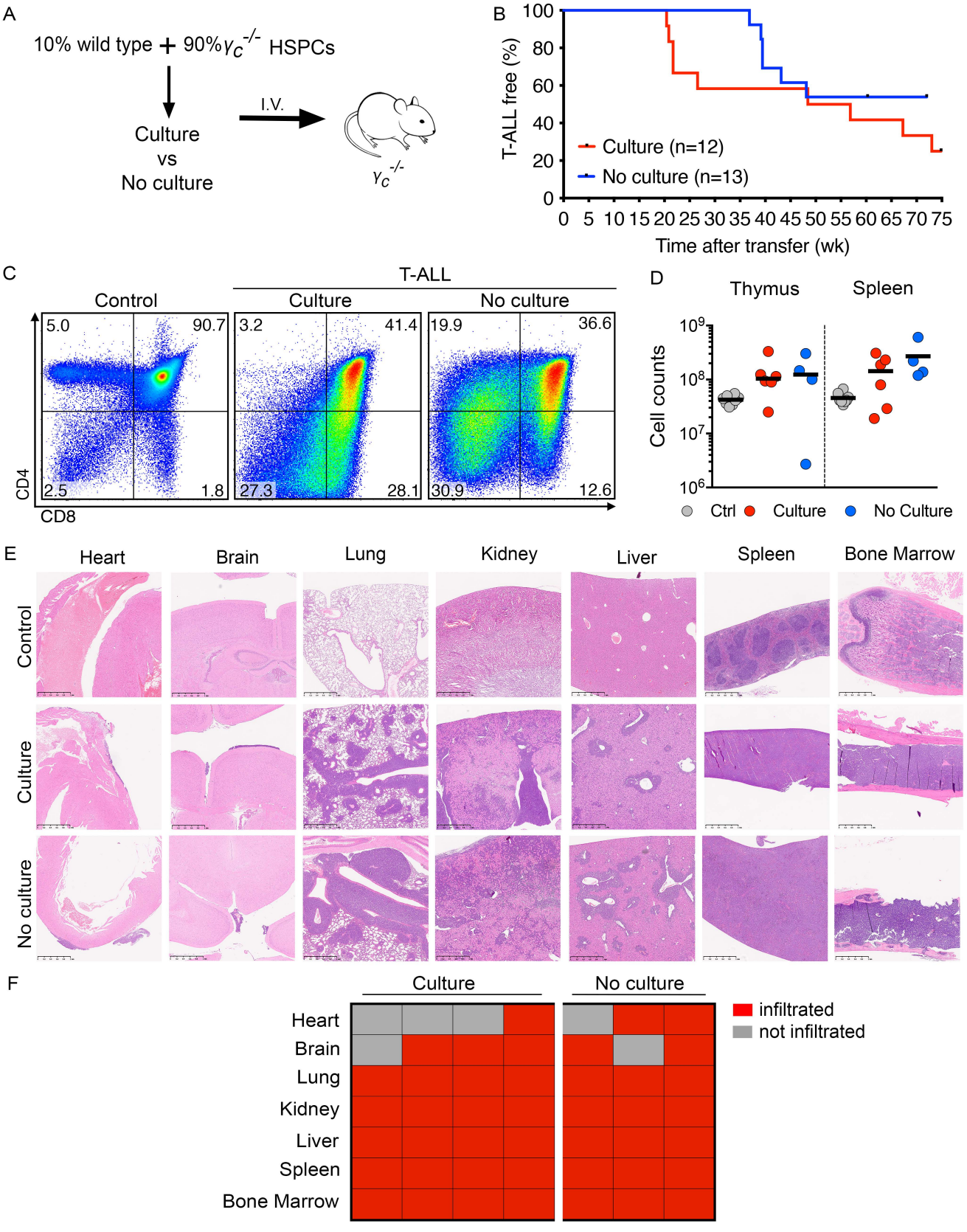
A
10% wild type + 90% γc-/- HSPCs
Culture
vs
No culture
I.V.
γc-/-
B
T-ALL free (%)
Culture (n=12)
No culture (n=13)
Time after transfer (wk)
C
T-ALL
Control
Culture
No culture
5.0
90.7
2.5
1.8
3.2
41.4
27.3
28.1
19.9
36.6
30.9
12.6
CD4
CD8
D
Thymus
Spleen
Cell counts
Ctrl
Culture
No Culture
E
Heart
Brain
Lung
Kidney
Liver
Spleen
Bone Marrow
Control
Culture
No culture
F
Culture
No culture
Heart
Brain
Lung
Kidney
Liver
Spleen
Bone Marrow
infiltrated
not infiltrated

Figure 2

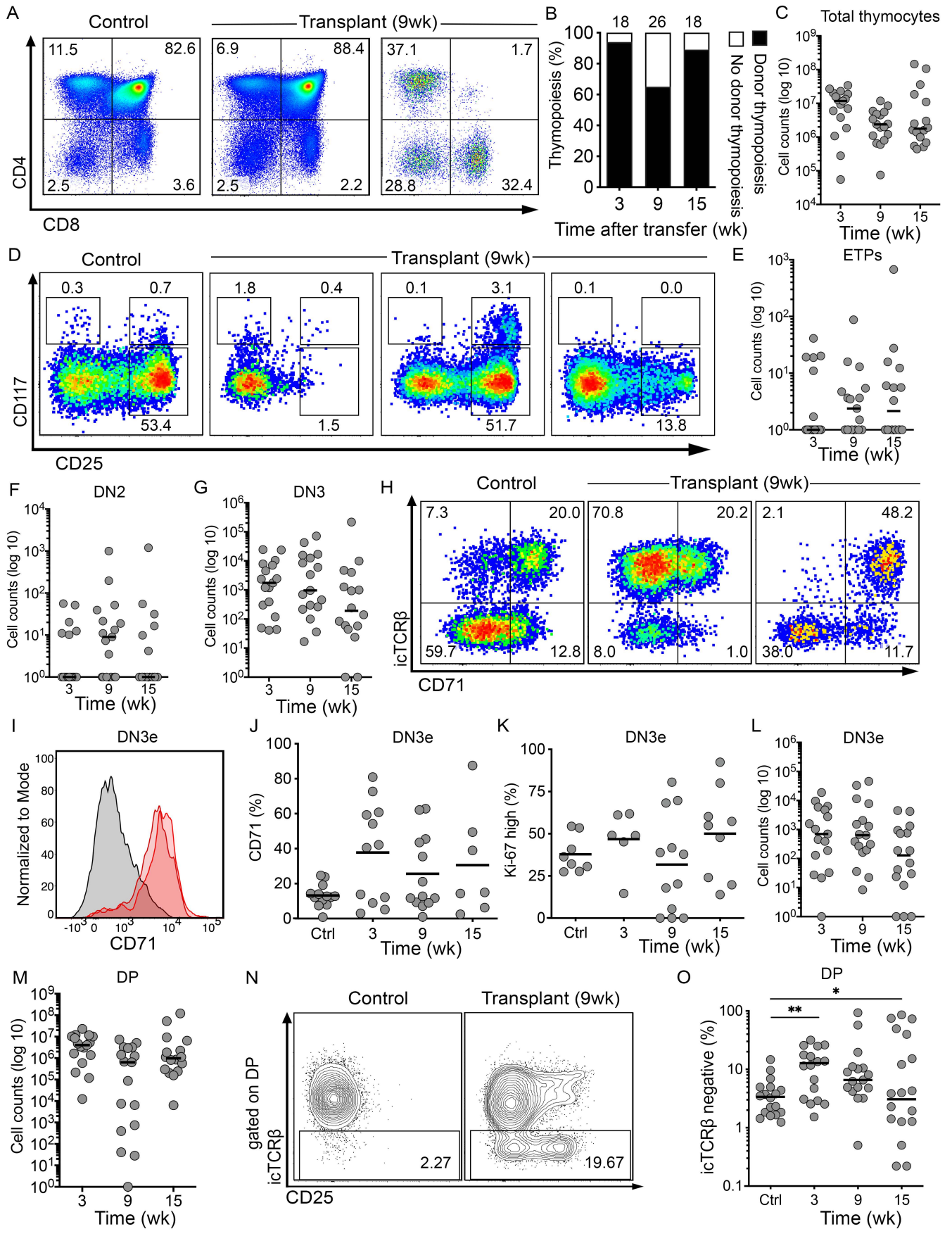
A
Control
Transplant (9wk)
11.5
82.6
2.5
3.6
6.9
88.4
2.5
2.2
37.1
1.7
28.8
32.4
CD4
CD8
B
18
26
18
Thymopoiesis (%)
No donor thymopoiesis
Donor thymopoiesis
Time after transfer (wk)
C
Total thymocytes
Cell counts (log 10)
Time (wk)
D
Control
Transplant (9wk)
0.3
0.7
53.4
1.8
0.4
1.5
0.1
3.1
51.7
0.1
0.0
13.8
CD117
CD25
E
ETPs
Cell counts (log 10)
Time (wk)
F
DN2
Cell counts (log 10)
Time (wk)
G
DN3
Cell counts (log 10)
Time (wk)
H
Control
Transplant (9wk)
7.3
20.0
59.7
12.8
70.8
20.2
8.0
1.0
2.1
48.2
38.0
11.7
icTCRβ
CD71
I
DN3e
Normalized to Mode
CD71
J
DN3e
CD71 (%)
Ctrl
Time (wk)
K
DN3e
Ki-67 high (%)
Ctrl
Time (wk)
L
DN3e
Cell counts (log 10)
Time (wk)
M
DP
Cell counts (log 10)
Time (wk)
N
Control
Transplant (9wk)
gated on DP
icTCRβ
2.27
19.67
CD25
O
DP
**
*
icTCRβ negative (%)
Ctrl
Time (wk)

Figure 3

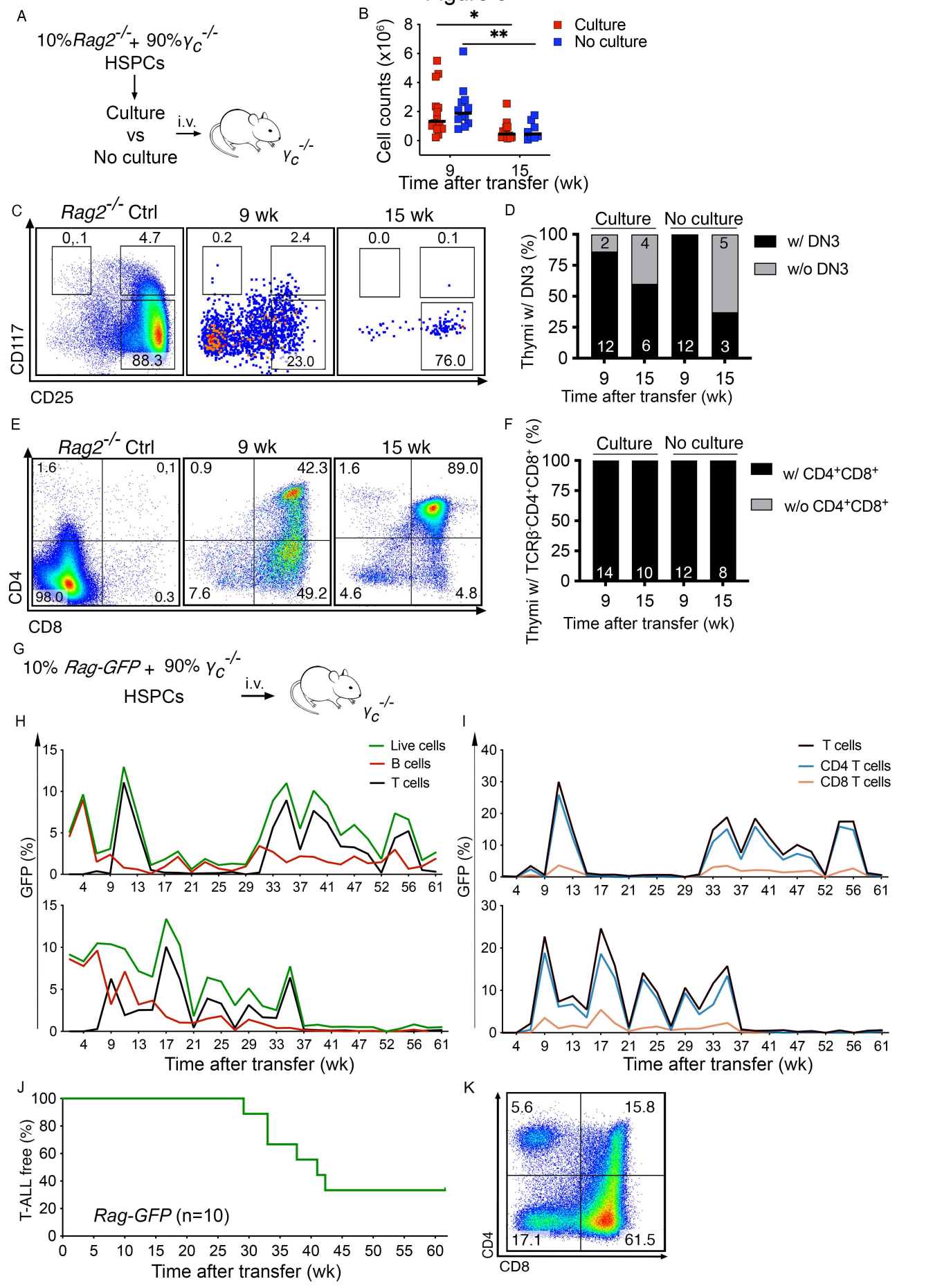
A
10%Rag2-/- + 90%γc-/- HSPCs
Culture vs No culture
i.v.
γc-/-
B
Cell counts (x10^6)
Culture
No culture
Time after transfer (wk)
C
Rag2-/- Ctrl
9 wk
15 wk
CD117
CD25
D
Culture
No culture
Thymi w/ DN3 (%)
w/ DN3
w/o DN3
Time after transfer (wk)
E
Rag2-/- Ctrl
9 wk
15 wk
CD4
CD8
F
Culture
No culture
Thymi w/ TCRβ-CD4+CD8+ (%)
w/ CD4+CD8+
w/o CD4+CD8+
Time after transfer (wk)
G
10% Rag-GFP + 90% γc-/- HSPCs
i.v.
γc-/-
H
Live cells
B cells
T cells
GFP (%)
Time after transfer (wk)
I
T cells
CD4 T cells
CD8 T cells
GFP (%)
Time after transfer (wk)
J
T-ALL free (%)
Rag-GFP (n=10)
Time after transfer (wk)
K
CD4
CD8

Figure 4

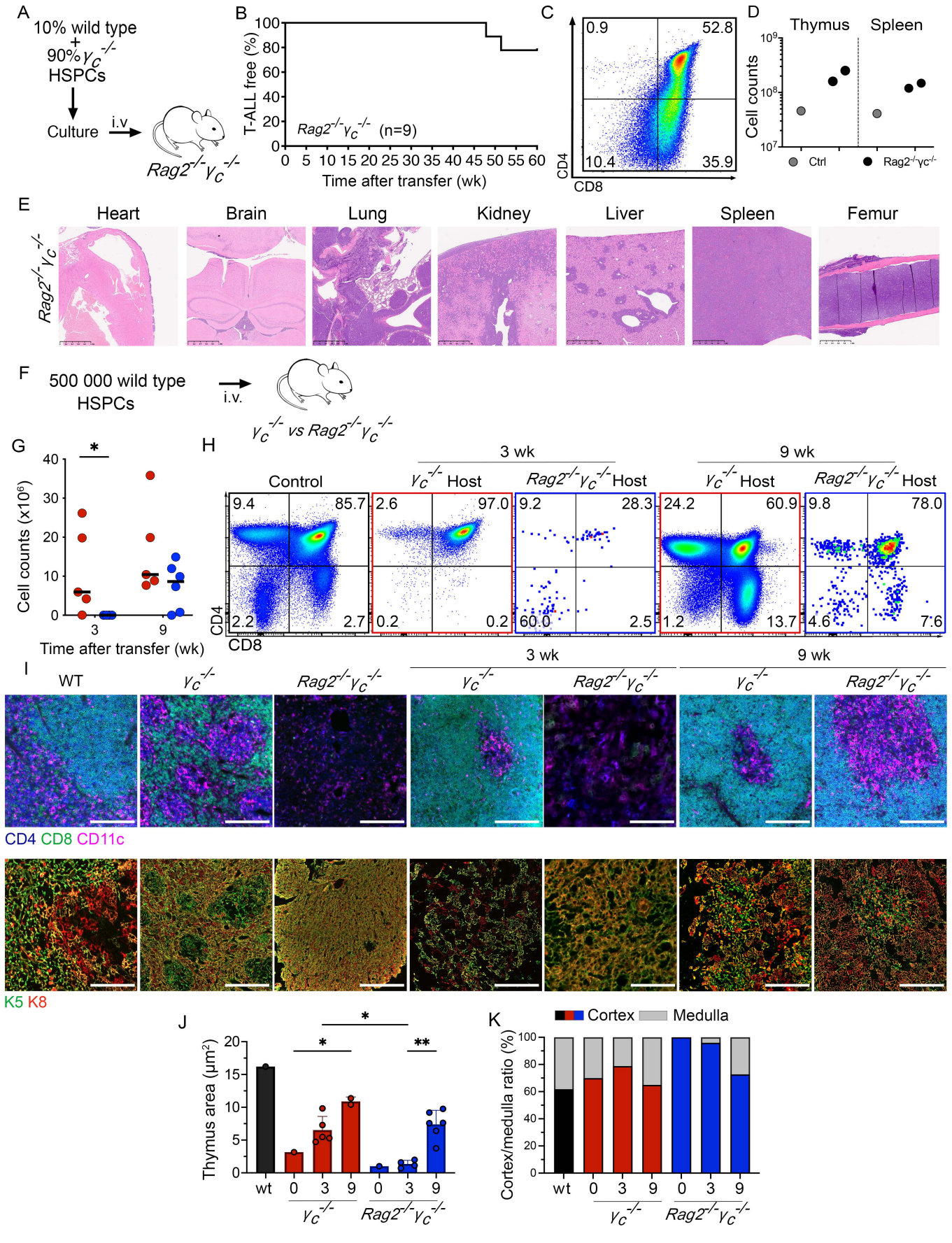
A
10% wild type
+
90% γc-/- HSPCs
Culture
i.v
Rag2-/-γc-/-
B
T-ALL free (%)
Rag2-/-γc-/- (n=9)
Time after transfer (wk)
C
0.9
52.8
10.4
35.9
CD4
CD8
D
Thymus
Spleen
Cell counts
Ctrl
Rag2-/-γc-/-
E
Heart
Brain
Lung
Kidney
Liver
Spleen
Femur
Rag2-/-γc-/-
F
500 000 wild type HSPCs
i.v.
γc-/- vs Rag2-/-γc-/-
G
Cell counts (x10^6)
Time after transfer (wk)
H
3 wk
9 wk
Control
γc-/- Host
Rag2-/-γc-/- Host
9.4
85.7
2.2
2.7
2.6
97.0
0.2
0.2
9.2
28.3
60.0
2.5
24.2
60.9
1.2
13.7
9.8
78.0
4.6
7:6
CD4
CD8
I
WT
γc-/-
Rag2-/-γc-/-
3 wk
9 wk
CD4 CD8 CD11c
K5 K8
J
Thymus area (μm²)
wt
0
3
9
γc-/-
Rag2-/-γc-/-
K
Cortex
Medulla
Cortex/medulla ratio (%)

Figure 5

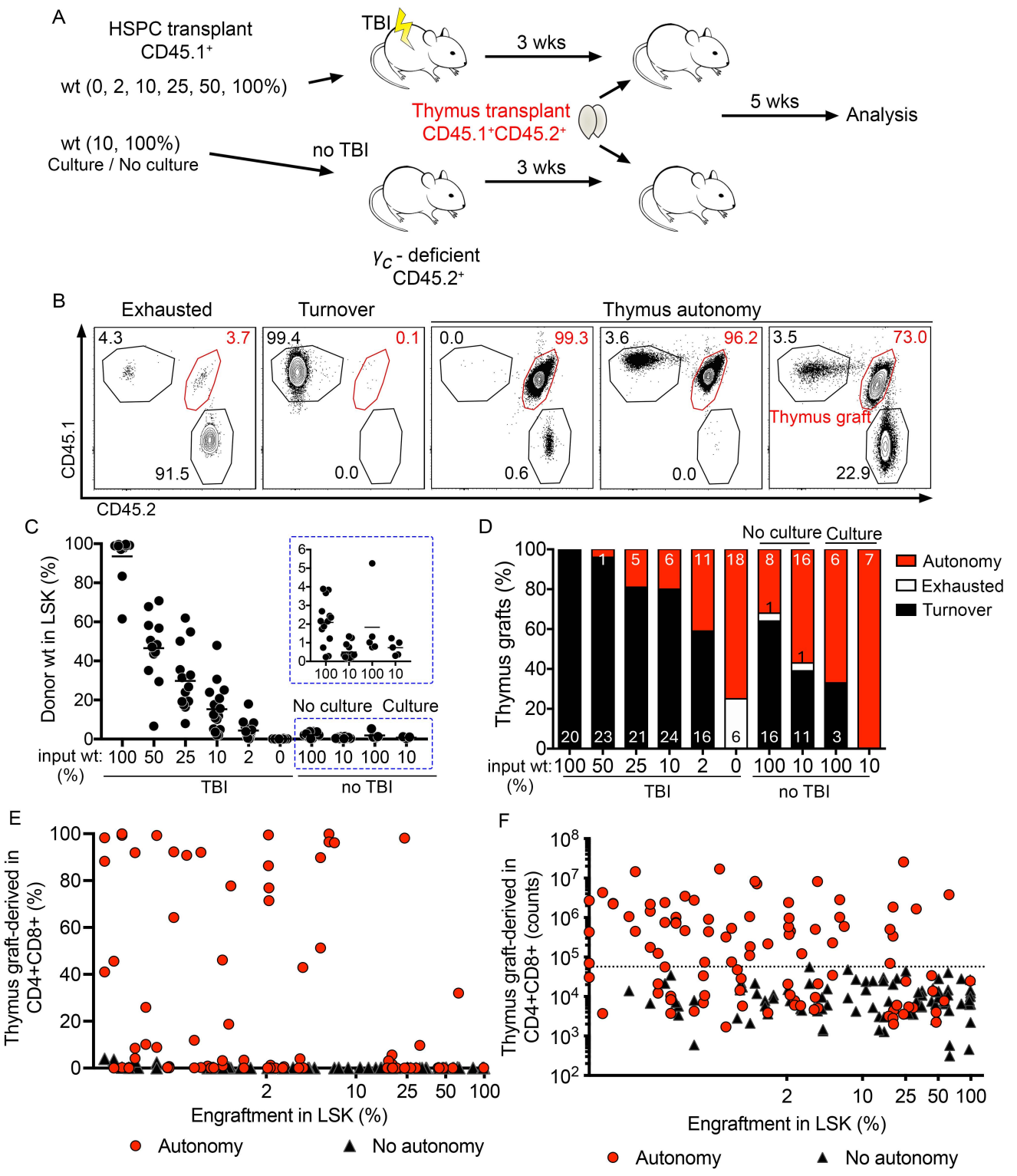
A
HSPC transplant
CD45.1+
wt (0, 2, 10, 25, 50, 100%)
TBI
3 wks
Thymus transplant
CD45.1+CD45.2+
5 wks
Analysis
wt (10, 100%)
Culture / No culture
no TBI
3 wks
γc - deficient
CD45.2+
B
Exhausted
Turnover
Thymus autonomy
4.3
3.7
91.5
99.4
0.1
0.0
0.0
99.3
0.6
3.6
96.2
0.0
3.5
73.0
Thymus graft
22.9
CD45.1
CD45.2
C
Donor wt in LSK (%)
input wt: (%)
100 50 25 10 2 0 100 10 100 10
TBI
no TBI
No culture Culture
D
Thymus grafts (%)
No culture Culture
Autonomy
Exhausted
Turnover
input wt: (%)
100 50 25 10 2 0 100 10 100 10
TBI
no TBI
E
Thymus graft-derived in CD4+CD8+ (%)
Engraftment in LSK (%)
Autonomy
No autonomy
F
Thymus graft-derived in CD4+CD8+ (counts)
Engraftment in LSK (%)
Autonomy
No autonomy